



## Artificial intelligence–based deep learning model for evaluating procedural consistency in microvascular anastomosis

Jiuxu Chen, MS,<sup>1,2</sup> Thomas J. On, BS,<sup>1</sup> Yuan Xu, MD,<sup>1</sup> Jonathan A. Tangsrivimol, MD,<sup>1</sup> Kivanc Yangi, MD,<sup>1</sup> Rokuya Tanikawa, MD,<sup>3</sup> Michael T. Lawton, MD,<sup>1</sup> Marco Santello, PhD,<sup>4</sup> Baoxin Li, PhD,<sup>2</sup> and Mark C. Preul, MD<sup>1</sup>

<sup>1</sup>The Loyal and Edith Davis Neurosurgical Research Laboratory, Barrow Neurological Institute, St. Joseph's Hospital and Medical Center, Phoenix, Arizona; <sup>2</sup>School of Computing and Augmented Intelligence, Arizona State University, Tempe, Arizona;

<sup>3</sup>Department of Neurosurgery, Sapporo Teishinkai Hospital, Sapporo, Hokkaido, Japan; and <sup>4</sup>School of Biological and Health Systems Engineering, Arizona State University, Tempe, Arizona

**OBJECTIVE** Assessing the consistency and precision of microanastomosis performance is crucial in neurosurgical training. Traditional methods rely on expert observation, which can be subjective and time-consuming. The aim of this study was to develop and validate a deep learning model using long short-term memory (LSTM) architecture for objective evaluation of microanastomosis performance by predicting and comparing suturing executions.

**METHODS** An LSTM-based neural network was developed to model and predict hand movements during microvascular anastomosis simulation. Video data were collected from 2 expert neurosurgeons performing microanastomosis twice, 1 year apart (sessions 1 and 2). Surgeon 1 performed interrupted suturing, and surgeon 2 performed continuous suturing. Additionally, a trainee with minimal microsurgical experience performed the interrupted suturing procedure once. Model performance was quantitatively assessed by comparing predicted and actual suturing executions using Kullback-Leibler (KL) divergence. Economy and flow of motion were also analyzed.

**RESULTS** The LSTM-based model accurately predicted suturing movements. Surgeon 1 demonstrated KL divergence values of 0.00063 (session 1) and 0.00061 (session 2), and surgeon 2 had values of 0.00082 (session 1) and 0.00016 (session 2). The trainee exhibited higher KL divergence (0.00196), reflecting less consistent performance. The economy of motion was assessed, showing mean Euclidean distances of 7.41 mm (session 1) and 5.85 mm (session 2) for surgeon 1, 10.53 mm (session 1) and 14.46 mm (session 2) for surgeon 2, and 10.50 mm for the trainee. The flow of motion analysis indicated median time intervals between sutures of 31.96 seconds (session 1) and 29.57 seconds (session 2) for surgeon 1, 21.53 seconds (session 1) and 21.50 seconds (session 2) for surgeon 2, and 101.23 seconds for the trainee.

**CONCLUSIONS** The LSTM-based model objectively assessed microanastomosis performance, capturing consistency and efficiency. Economy and flow of motion metrics were further validated. Future studies will extend the model's application to more surgeons and refine interpretation of the performance metrics.

<https://thejns.org/doi/abs/10.3171/2025.6.JNS25128>

**KEYWORDS** artificial intelligence; deep learning; hand landmarks; hand tracking; microanastomosis; microvascular anastomosis; neurosurgical training; vascular disorders

**M**ICROVASCULAR anastomosis is an exacting and specialized neurosurgical technique requiring highly refined movements that predominantly engage the intrinsic muscles of the hands.<sup>1</sup> Given the technical difficulty of microvascular anastomosis, trainees must practice and develop their anastomosis skills in

simulation laboratories before performing the procedure in a clinical setting.<sup>2</sup>

Standardized and nonstandardized assessment methods have been developed for microsurgical simulation training. However, these methods rely on skilled mentors to assess technical performance based on specific parameters,

**ABBREVIATIONS** AI = artificial intelligence; CNN = convolutional neural network; DL = deep learning; KL = Kullback-Leibler; LSTM = long short-term memory; MAD = median absolute deviation; SEM = standard error of the mean.

**SUBMITTED** January 21, 2025. **ACCEPTED** June 27, 2025.

**INCLUDE WHEN CITING** Published online September 26, 2025; DOI: 10.3171/2025.6.JNS25128.

which is inconvenient and impractical in real-life scenarios.<sup>3</sup> To address these limitations, automated assessment tools have been developed using electromagnetic trackers on the dorsum of microsurgeons' hands coupled with software to capture hand motions and calculate movement distances.<sup>4</sup> Despite validation,<sup>5–8</sup> the limitations of physical sensors include reduced accuracy due to sensor shift, restricted flexibility, unnatural movements from bands and wires, and high expense.

Recent advancements in artificial intelligence (AI) have led to the development of the MediaPipe Hand Landmarker (Google AI), a pretrained convolutional neural network (CNN) that can detect the movements of 21 hand landmarks without needing physical sensors on the hand.<sup>9</sup> Adaptation of this model has enabled assessment of trainees during microsurgical simulations by analyzing parameters, such as the economy, amplitude, and flow of motion, based on hand landmark data.<sup>10–12</sup> However, there are still no well-defined metrics for determining consistency across suturing executions or for predicting the appearance and characteristics of the next sutures.

Therefore, we aimed to develop an AI-driven model using deep learning (DL) techniques to assess the consistency of hand motion during microvascular anastomosis, and to validate the accuracy and reliability of the individualized models in predicting and quantifying surgical motion with expert surgeons while providing preliminary comparisons with trainee performance. Our approach uses surgeon-specific neural network models based on surgical movements captured from 2 expert cerebrovascular-specialized neurosurgeons (M.T.L. and R.T.), as well as a trainee with minimal microsurgical experience, performing microanastomosis simulations.

## Methods

### Experimental Design

During 2 separate cerebrovascular surgery courses held 1 year apart, 2 expert cerebrovascular-specialized neurosurgeons performed microanastomosis simulations. Surgeon 1 executed end-to-side anastomosis using an interrupted technique with a fish-mouth linear arteriotomy, with the recipient vessel oriented vertically and stabilized. Surgeon 2 executed the same procedure using a continuous technique. Each surgeon performed their respective procedures once at each course, resulting in 2 separate recordings per surgeon. Additionally, to provide a comparative reference to the preliminary expert results, we separately recorded a trainee with minimal microsurgical experience performing the same simulation under identical experimental conditions using an interrupted suturing technique.

We recorded videos of the surgeons performing the simulation using the same experimental design as in our previous work (Fig. 1).<sup>10,11</sup> Anastomosis procedures were performed on 2-mm diameter polyvinyl alcohol vessels (Micro Vascular Model, EXSURG) using appropriate microsurgical instruments, an adjustable surgical table, and a chair with armrests and foot pedals.

Videos of the anastomosis simulation were recorded using an action camera (GoPro), positioned 450 mm from



**FIG. 1.** Illustration showing the experimental setup of the DL tracking system for microanastomosis simulation. The operator performs anastomosis simulation under the operative microscope while an action camera records the simulation. The video feed is processed in real time through the hand detection model, which provides annotation of hand movements as displayed on the computer screen. Used with permission from Barrow Neurological Institute, Phoenix, Arizona. Figure is available in color online only.

the table edge. Videos were then processed with the pretrained MediaPipe Hand Landmarker task, a CNN-based application that estimates the 2D coordinates of 21 hand landmarks in each frame. We used a Nvidia GeForce RTX 3060 laptop GPU and an Intel Core i7-11800h laptop CPU for all our experiments. The output from the MediaPipe hand-tracking algorithm is a large numerical matrix containing the spatial coordinates (x, y) of each landmark, indexed by joint position and hand (left or right) for each recorded frame. This numerical matrix served as input data for subsequent algorithmic analyses and DL-based performance metrics. Additionally, MediaPipe outputs an annotated video visually displaying the labeled joints as a representation of this numerical matrix (Video 1).

**VIDEO 1.** Video showing real-time AI tracking of hand movements during end-to-side microanastomosis performed using a continuous suturing technique. The MediaPipe Hand Landmarker labels 21 blue landmarks on each hand corresponding to finger joints and wrist, annotating hand motions of the surgeon throughout the procedure. Used with permission from Barrow Neurological Institute, Phoenix, Arizona. Click here to view.

### Algorithmic Analysis of Hand Movement Metrics

#### Economy of Motion

Economy of motion was defined as precise and purposeful instrument handling with minimal extraneous movements.<sup>11</sup> To quantify this metric, we measured the average movement (in pixels) of the surgeon's dominant-hand second-digit tip relative to a baseline position, de-

fined as the median coordinate location during suturing. This method is logical because smaller deviations from this central reference point reflect more controlled and deliberate movements. To isolate movements directly related to the suturing technique, we applied an outlier detection algorithm that assigned an anomaly score to each data point. An anomaly score quantifies how much a data point deviates from the central tendency of the dataset. Scores greater than 3.5, representing significant movements unrelated to suturing (e.g., suture cutting or instrument exchanges), were excluded. Subsequently, horizontal (x-axis) and vertical (y-axis) tracking data were converted into Euclidean distances relative to the median baseline position. Distances were calculated using the calibration of 1 pixel corresponding to 2.51 mm at the depth of the surgeon's hand. The mean Euclidean distance and standard error of the mean (SEM) were calculated to generate economy of motion scores.

#### Flow of Motion

Flow of motion was defined as the speed and temporal efficiency of suturing movements.<sup>11</sup> Using a peak detection algorithm from SciPy (version 1.15.1),<sup>13</sup> we identified significant peaks in vertical movements of the dominant hand's index finger. Each detected peak corresponded to an individual suture pass, with notably large amplitude peaks indicating instrument exchanges and suture cutting during interrupted suturing, or suture pulls during continuous suturing. The intervals between these large-amplitude peaks were measured and used to calculate the median time per suture, representing the speed of each surgeon's suturing performance. The time intervals for each suture were calculated, and the median and median absolute deviation (MAD) were reported for each session.

#### Deep Neural Network Model for Training and Predicting

We used a deep neural network, specifically a long short-term memory (LSTM) network,<sup>14</sup> to objectively evaluate individual surgeon microanastomosis performance. A common machine learning approach involves dividing data into training and testing segments, where a model learns patterns from one portion (training data) and then predicts unseen movements in another segment (testing data). Accordingly, for each surgeon, we trained a separate LSTM neural network using approximately the last 75% of their recorded suturing movements (training data). After this training phase, the model received the initial 25% of that surgeon's recorded movements (testing data) and predicted subsequent suturing patterns.

The logic behind this approach is that if a surgeon demonstrates consistent and skilled technique during the majority (75%) of their performance, these characteristic patterns should be reliably reflected in the initial portion (25%) of the same procedure. Thus, a skilled and consistent surgeon's actual suturing movements should closely match the model's predictions. We quantitatively assessed the match between predicted and actual suturing movements using Kullback-Leibler (KL) divergence, a statistical metric measuring similarity. Lower KL divergence values indicated higher similarity between the predicted and actual suturing patterns, reflecting greater skill and consistency.

To generate the training data, we randomly selected 400 short clips (each comprising 5% of the total video length) from the final 75% of each surgeon's video using the numerical matrix from MediaPipe Hand Landmarker that provided spatial coordinates (x, y) of 21 distinct hand landmarks per frame. The subsequent 5% of frames following each selected clip served as corresponding training labels, guiding the model to learn sequential patterns in hand movements. This randomized selection was repeated at each training epoch to enhance the model's generalization.

Our neural network architecture consisted of an input fully connected layer (256 hidden units), 2 consecutive LSTM layers (each with 512 hidden units), and an output fully connected layer (256 hidden units). The network was trained to optimize prediction accuracy by minimizing the mean squared error between predicted movements and actual recorded movements.

## Results

Each expert surgeon performed the simulation twice in separate sessions that were 1 year apart (session 1 and session 2). In session 1, surgeon 1 had 525,714 landmark detections with a tracking loss of 7.32%, and surgeon 2 had 717,066 landmark detections with a tracking loss of 0.21%. In session 2, surgeon 1 had 855,120 landmark detections with a tracking loss of 0.14%, and surgeon 2 had 734,580 landmark detections with a tracking loss of 7.30%. The trainee performed the simulation once, recording 2,524,872 landmark detections with a tracking loss of approximately 0.28%. The AI motion detection model identified x and y coordinate positions for each landmark detection, which were used to construct motion graphs illustrating movements across horizontal and vertical planes.

#### Video Annotation and Correlation With Tracking

In microanastomosis, the second digit of the dominant hand commonly manipulates the instrument, whereas the fifth digit provides stability and support. Our analysis focused on these 2 digits because they can be generalized to represent the hand's surgical movements. The microscope video feed and hand motion data were captured simultaneously for each simulation. Amplitude changes in the motion graphs correlated with the corresponding surgical actions observed in the video recordings.

For surgeon 1 (Fig. 2), who performed the anastomosis simulation using an interrupted suturing technique, small amplitude changes in the horizontal motion graph correlated with suture pulls. Larger double-peaks in the same graph correlated with instrument changes; specifically, transitions from microforceps to microscissors for suture cutting and then switching back to microforceps for the next stitch. Similarly, the vertical motion graph displayed peaks at corresponding time points reflecting these gross movements. The tracking data remained consistent when comparing results from sessions 1 and 2. The trainee, who also performed interrupted suturing, exhibited a motion graph shape generally similar to that of surgeon 1, characterized by repetitive larger amplitude movements associ-

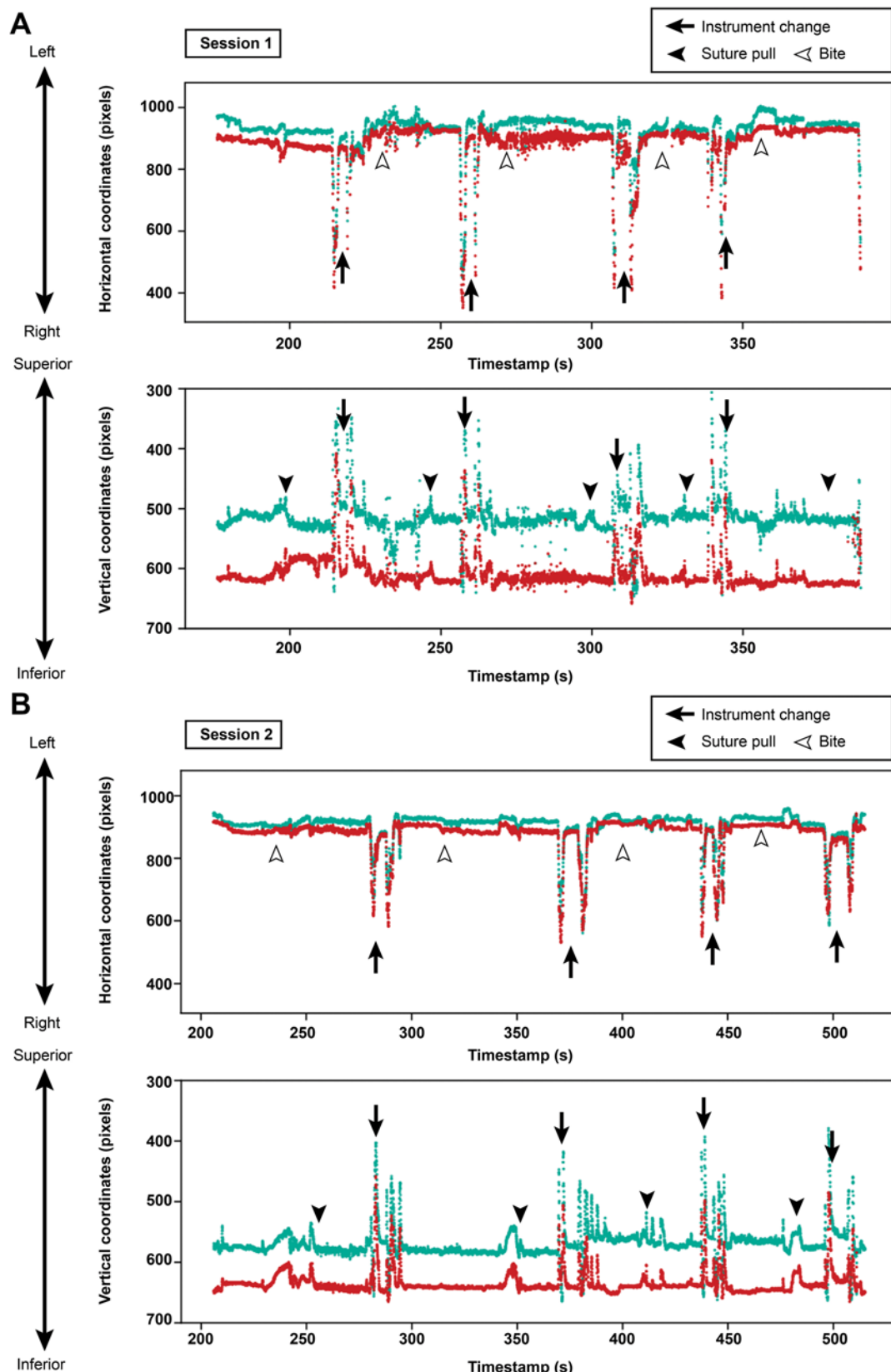


**FIG. 2.** Motion graphs showing tracking data for surgeon 1 in session 1 (A) and session 2 (B). The tips of the second (teal) and fifth (red) digits were analyzed while the surgeon performed end-to-side anastomosis using an interrupted suturing technique with a fish-mouth linear arteriotomy and vertical orientation of the recipient vessel. Notable amplitude changes are visible, which correlate with specific surgical actions during the procedure. Figure is available in color online only.

ated with frequent instrument exchanges during the interrupted suturing technique.

For surgeon 2 (Fig. 3), who performed the anastomosis simulation using the continuous suturing technique, fewer large movements were observed due to the lack of instrument changes. Low amplitude movement was evident in the tracking data from sessions 1 and 2, which demonstrated a consistent narrower interval rhythm that correlated with suture pulls. Surgeon 2 also exhibited a distinct dip at the peak of the tracking data, which indicated a consistent mid-suture pull adjustment to reposition the suture loop with the nondominant hand. However, this pattern was more pronounced in the vertical tracking data.

### Economy and Flow of Motion

Economy of motion was evaluated by analyzing the mean and SEM micromovement of each surgeon's dominant hand relative to their baseline position during suturing. Lower values indicate a reduced amplitude of movement, which reflects less excess motion. For surgeon 1, the mean Euclidean distance was 7.41 (SEM 0.039) mm in session 1 and 5.85 (SEM 0.031) mm in session 2. For surgeon 2, the mean Euclidean distance was 10.53 (SEM 0.074) mm in session 1 and 14.46 (SEM 0.214) mm in session 2. For the trainee, the mean Euclidean distance was 10.50 (SEM 14.96) mm.

Flow of motion was assessed using a peak detection algorithm, which identified significant amplitude changes in the dominant hand's index finger during suturing. The median time interval between sutures for surgeon 1 was 31.96 (MAD 10.98) seconds in session 1 and 29.57 (MAD 14.60) seconds in session 2. Surgeon 2 had median intervals of 21.53 (MAD 0.74) seconds in session 1 and 21.50 (MAD 1.42) seconds in session 2. For the trainee, the median interval was 101.23 (MAD 11.36) seconds.

### Prediction of Suturing Model Performance

Horizontal and vertical motion graphs visualize the DL model's ability to predict and track suturing movements. The model accurately captured the movement patterns, including large amplitude changes, for both surgeons. For surgeon 1, the KL divergence was 0.00063 in session 1 and 0.00061 in session 2 (Fig. 4). Surgeon 2 had a KL divergence of 0.00082 in session 1 and 0.00016 in session 2 (Fig. 5). The trainee had a KL divergence of 0.00196 (Fig. 6).

## Discussion

In microanastomosis, both interrupted and continuous suturing follow the same initial steps. The "bite" involves the needle penetrating the arterial wall perpendicularly, followed by the "suture pull," in which the microforceps grasp the needle to pull the suture through. In interrupted suturing, a knot is tied after each suture to secure the vessels, with frequent instrument changes between the needle driver and scissors. In contrast, continuous suturing involves a single uninterrupted suture line with a final knot at the end, thereby reducing the number of instrument changes.

Manual annotation and comparison of tracking data in

surgical simulations are feasible but are often time-consuming and subject to human error. In contrast, algorithmic or AI analysis of objective tracking data provides a more efficient and objective method for evaluating changes in performance. Taking advantage of the repetitive actions used during microanastomosis, we first tested our previously described methods<sup>11</sup> to evaluate the economy and flow of motion. Subsequently, we used an AI judge to predict the expected microanastomosis execution, which was trained on the actual performance of the trainee in the microanastomosis simulation as the skill representation. We determined the consistency of motion for an expert neurosurgeon or trainee by computing the difference (KL divergence) between the expected execution and the ground truth execution.

Our results showed a high degree of similarity in performance from year to year for each expert neurosurgeon, as reflected in the closely matched economy of motion, flow of motion, and KL divergence values across simulations. The economy of motion analysis demonstrated minimal hand movement during the anastomosis procedure, which is expected when suturing small vessels. Notably, the flow of motion analysis showed almost identical results for each surgeon across years, although not between surgeons. The continuous suturing technique took less time between bites compared with the interrupted technique. The AI model's low KL divergence values for both surgeons indicated strong consistency within each simulation, with minimal variation in technique throughout the procedure.

Compared with the surgeons, the trainee demonstrated less consistent performance overall, which was indicated by a higher KL divergence value, longer intervals between sutures (flow of motion), and a mean amplitude of hand movement (economy of motion) similar to that of surgeon 1 but with substantially greater variability. These findings suggest that trainees can achieve similar magnitudes of movement primarily because microsurgical procedures performed under a microscope inherently constrain movement to a small, focused target area. However, trainees typically lack the precision, efficiency, and rhythmic pacing that are characteristic of expert surgeons due to their developing motor skills and limited procedural experience.

Our algorithmic and DL-based assessment method could be practically integrated into microanastomosis training courses by recording trainees as they perform microanastomosis tasks during simulations. Although a GoPro camera was used in this study, relatively simple recording equipment, such as a smartphone camera, would suffice. Participants' motions could be tracked multiple times during a course. These recordings could then be efficiently analyzed through an automated computational pipeline developed in Python, which processes hand landmark data to calculate essential performance metrics, such as the economy of motion, flow of motion, and KL divergence. This streamlined approach allows performance analyses for multiple trainees to be completed within a single day, although the actual processing time might vary depending on workstation specifications, including GPU capabilities, CPU speed, and available RAM.

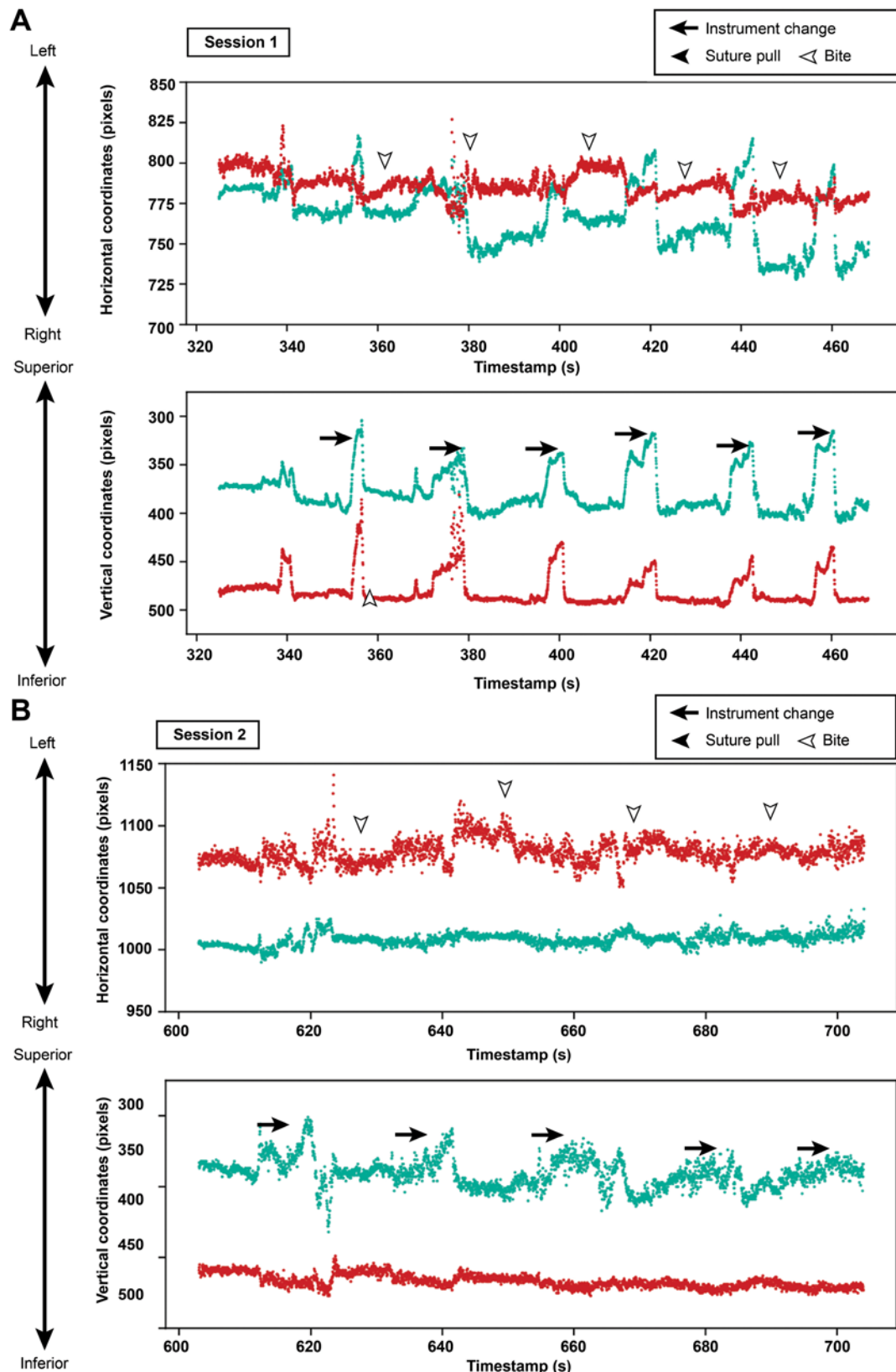


**FIG. 3.** Motion graphs showing tracking data for surgeon 2 in session 1 (A) and session 2 (B). The tips of the second (teal) and fifth (red) digits were analyzed while the surgeon performed end-to-side anastomosis using a continuous suturing technique with a fish-mouth excision arteriotomy and an oblique orientation of the recipient vessel. Notable amplitude changes are visible, which correlate with specific surgical actions during the procedure. Figure is available in color online only.

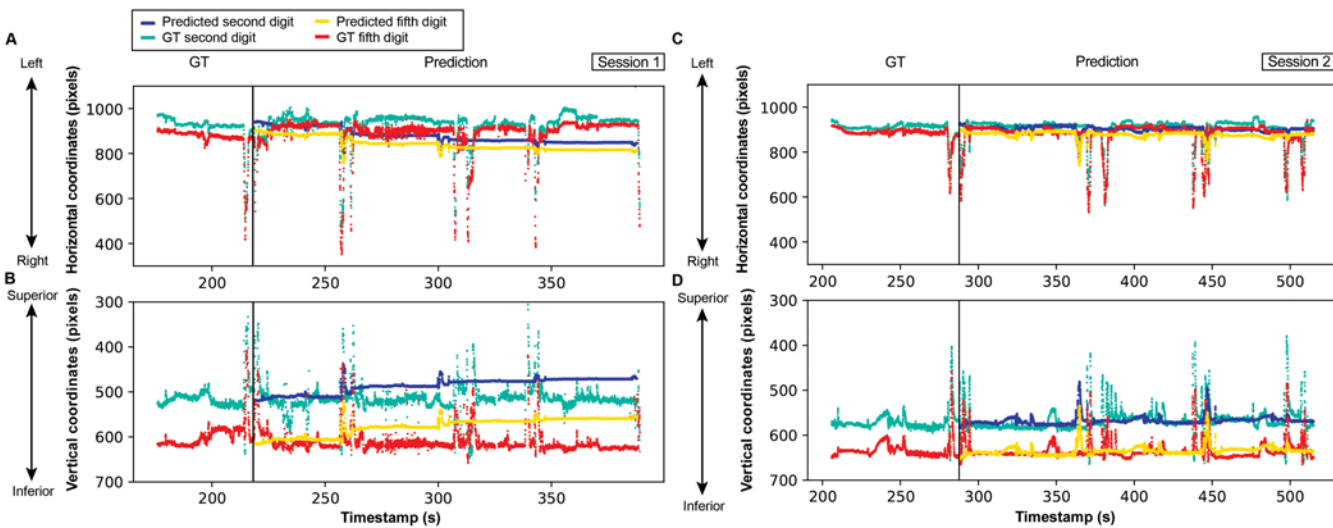


**FIG. 4.** Motion graphs showing the LSTM network's predicted execution for surgeon 1 compared with the ground truth (GT) for horizontal (A) and vertical (B) coordinates in session 1 and horizontal (C) and vertical (D) coordinates in session 2. Figure is available in color online only.

In practical training scenarios, trainees can perform microanastomosis simulations over several days and objectively track their skill progression by monitoring the KL divergence. Improved performance in microanastomosis is reflected by decreasing KL divergence values over time. Additionally, differences in KL divergence values between trainees offer a quantifiable comparison of their respective skill levels. A study is currently underway to evaluate the applicability and effectiveness of this system for objectively monitoring neurosurgery trainees' skill progression.

### Rationale for DL Architecture

We deployed a deep neural network architecture to model the temporal transitions of hand landmark detec-

tions and serve as our AI judge for assessment of microanastomosis performance. Recent studies have shown that CNN-based architectures, particularly those with stacks of inception modules, can model complex temporal transitions in video data.<sup>15,16</sup> However, CNNs are primarily designed to capture spatial patterns within images, making them less optimal for tasks focused on temporal dynamics.<sup>17</sup> Transformers,<sup>18</sup> known for their superior temporal modeling compared with recurrent neural network-based architectures, have become popular and have proved successful in various tasks. Nonetheless, a transformer's performance can diminish when required to handle extremely long sequences, such as those exceeding 20 minutes in microanastomosis simulation videos. This limitation can be addressed by reorganizing frame-by-frame action labels

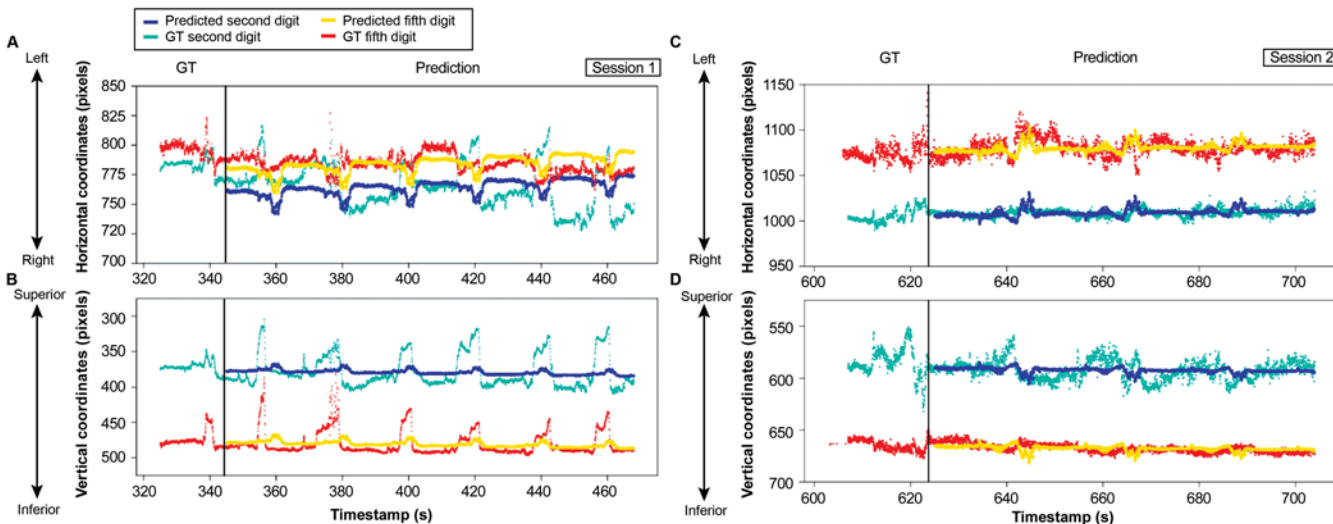


**FIG. 5.** Motion graphs showing the LSTM network's predicted execution for surgeon 2 compared with the GT for horizontal (A) and vertical (B) coordinates in session 1 and horizontal (C) and vertical (D) coordinates in session 2. Figure is available in color online only.

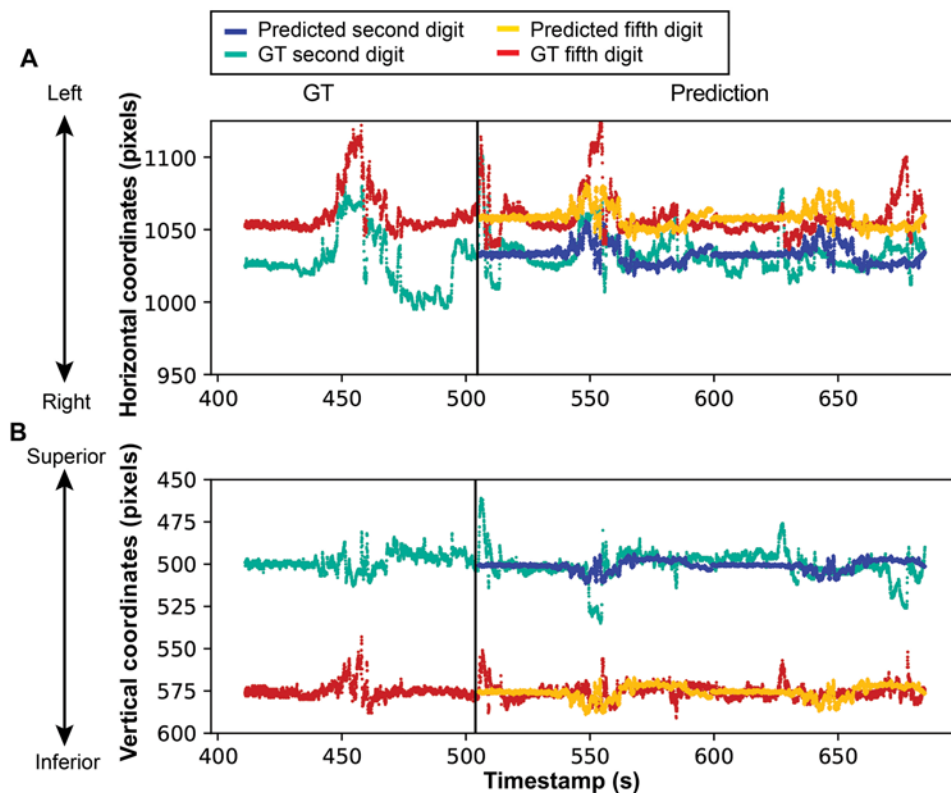


**FIG. 6.** Motion graphs showing the LSTM network's predicted execution for the trainee compared with the GT for horizontal (A) and vertical (B) coordinates. Figure is available in color online only.

into action segments with multiple frames and their durations.<sup>19–22</sup> However, because we cannot access fine-grained microanastomosis action annotations, implementing this approach was not feasible in our work.

Therefore, for this study, we chose the LSTM architecture, a specialized type of recurrent neural network.<sup>14</sup> LSTM networks are specifically engineered to overcome the limitations of traditional recurrent neural networks, such as the vanishing gradient problem, by introducing memory cells that can maintain and regulate information flow over long periods. The LSTM network's autoregressive prediction scheme also provides flexibility in designing the training protocol.

### DL Skill Assessment

If a trainee were to perform microanastomosis perfectly, all the suturing actions completed within a simulation would be the same. Consequently, the AI judge will be trained on samples containing identical patterns of hand landmark detections. If we pass a skill testing clip excerpted from any suturing sequence to the model, the AI judge should predict an expected skill representation that is identical to the actual execution, resulting in a KL divergence of 0. Therefore, a trained AI judge is well suited to predict a trainee's performance.

This design requires only 1 annotation per video to excerpt a complete suturing clip, thereby minimizing the need for manual annotation. Because the predicted expectation will always be the same length as the ground truth

execution, there is no need to tailor clips to be the same length for comparison. Additionally, replacing in-person supervision and assessment by microsurgery experts with an AI judge trained on the trainee's real performance mitigates potential bias in skill assessment.

By inputting a complete suturing sequence (i.e., a skill testing sample) into a trained deep neural network, the network predicted the expected execution. This expected execution was a sequence of 2D hand landmark trajectories representing what the AI judge anticipated a trainee to perform in the next several minutes after the input suturing sequence. This approach allowed objective measurement of the consistency of the trainee's suturing motions.

### Limitations

This study primarily focused on analyzing the suturing predictions of 2 expert cerebrovascular-specialized neurosurgeons. These experts were chosen to develop and test the model because their suturing patterns are more predictable and provide a reliable foundation for model training and validation. Each surgeon performed the continuous or interrupted suturing technique, respectively, allowing for a comprehensive analysis of both methods. However, to enhance the generalizability of our findings, the model would need to be tested on individuals whose movements are less predictable.

Quantification of KL divergence in the context of suturing patterns has not yet been firmly established and, as such, determining what constitutes a "good" or "bad" KL

divergence value will require analysis on a much larger dataset. Once we develop a metric system for evaluating KL divergence values, this metric can be used to assess changes in skill for individual surgeons over time and to compare skill levels between surgeons. Establishing such a standard will be crucial for objectively evaluating and comparing the microanastomosis proficiency of surgeons.

Hand motion is not the only factor in the successful performance of microanastomosis. Although precise and consistent hand movements are important, they do not fully capture the overall quality of the procedure. Assessment of the vessel and its patency is also necessary because a surgeon could perform with excellent hand movement but still experience poor outcomes as a result of improper suturing or vessel damage.

Only end-to-side anastomosis was performed in this study; therefore, other types of anastomoses need to be studied using this model to ensure broader applicability. Although measuring consistency in hand motion is valuable, it represents just one aspect of performance. Other AI models should be developed to examine additional aspects, such as the amplitude of movement and economy of motion, for a more comprehensive analysis of surgical technique.

Finally, the findings presented herein are strictly limited to a controlled simulation environment and might not be directly applicable to assess surgical skill during actual operative procedures. Performance dynamics in the operating room are influenced by real-world complexities, such as patient-specific anatomy, physiological conditions, stress, and intraoperative variability, and thus are beyond the scope of this simulation-based assessment.

## Conclusions

We developed and applied a DL model using LSTM architecture to assess microanastomosis performance based on the consistency of hand movements. By calculating the KL divergence between predicted and actual suturing executions, we demonstrated the model's potential to objectively evaluate the consistency of a neurosurgeon's technique. In addition to KL divergence, we further validated other algorithmic assessment methods, including the economy and flow of motion, which provided complementary insights into suturing precision and efficiency. Although the current analysis is limited to 2 experts and 1 trainee, future studies will expand the model's application to a broader range of surgeons and further refine the interpretation of these metrics in the context of suturing skill assessment.

## Acknowledgments

Funding for this study was provided by the Barrow Neurological Foundation to Dr. Preul. We thank the staff of Neuroscience Publications at Barrow Neurological Institute for assistance with manuscript and video preparation.

## References

1. Ramachandran S, Ghanem AM, Myers SR. Assessment of microsurgery competency—where are we now? *Microsurgery*. 2013;33(5):406-415.
2. Evgeniou E, Walker H, Gujral S. The role of simulation in microsurgical training. *J Surg Educ*. 2018;75(1):171-181.
3. Polavarapu HV, Kulaylat AN, Sun S, Hamed OH. 100 years of surgical education: the past, present, and future. *Bull Am Coll Surg*. 2013;98(7):22-27.
4. Grober ED, Hamstra SJ, Wanzer KR, et al. Validation of novel and objective measures of microsurgical skill: hand-motion analysis and stereoscopic visual acuity. *Microsurgery*. 2003;23(4):317-322.
5. Moulton CAE, Dubrowski A, Macrae H, Graham B, Grober E, Reznick R. Teaching surgical skills: what kind of practice makes perfect? A randomized, controlled trial. *Ann Surg*. 2006;244(3):400-409.
6. Saleh GM, Gauba V, Sim D, Lindfield D, Borhani M, Ghousayni S. Motion analysis as a tool for the evaluation of oculoplastic surgical skill: evaluation of oculoplastic surgical skill. *Arch Ophthalmol*. 2008;126(2):213-216.
7. Ezra DG, Aggarwal R, Michaelides M, et al. Skills acquisition and assessment after a microsurgical skills course for ophthalmology residents. *Ophthalmology*. 2009;116(2):257-262.
8. Grober ED, Roberts M, Shin EJ, Mahdi M, Bacal V. Intraoperative assessment of technical skills on live patients using economy of hand motion: establishing learning curves of surgical competence. *Am J Surg*. 2010;199(1):81-85.
9. Google. Hand Landmarks Detection Guide. Accessed July 11, 2025. [https://ai.google.dev/edge/mediapipe/solutions/vision/hand\\_landmarker](https://ai.google.dev/edge/mediapipe/solutions/vision/hand_landmarker)
10. Gonzalez-Romo NI, Hanalioglu S, Mignucci-Jiménez G, et al. Quantification of motion during microvascular anastomosis simulation using machine learning hand detection. *Neurosci Focus*. 2023;54(6):E2.
11. On TJ, Xu Y, Chen J, et al. Deep learning detection of hand motion during microvascular anastomosis simulations performed by expert cerebrovascular neurosurgeons. *World Neurosurg*. 2024;192:e217-e232.
12. On TJ, Xu Y, Gonzalez-Romo NI, et al. Detection of hand motion during cadaveric mastoidectomy dissections: a technical note. *Front Surg*. 2024;11:1441346.
13. Virtanen P, Gommers R, Oliphant TE, et al. SciPy 1.0: fundamental algorithms for scientific computing in Python. *Nat Methods*. 2020;17(3):261-272.
14. Graves A. Long short-term memory. In: *Supervised Sequence Labelling with Recurrent Neural Networks*. Springer Berlin Heidelberg; 2012:37-45.
15. Piergiovanni A, Angelova A, Toshev A, Ryoo MS. Evolving space-time neural architectures for videos. In: *Proceedings of the IEEE/CVF International Conference on Computer Vision*. IEEE; 2019.
16. Zhang D, Li C, Lin F, et al. Detecting deepfake videos with temporal dropout 3DCNN. In: *Proceedings of the Thirtieth International Joint Conference on Artificial Intelligence (IJCAI-21)*. IJCAI; 2021.
17. Gao Z, Tan C, Wu L, Li SZ. SimVP: simpler yet better video prediction. In: *Proceedings of the IEEE/CVF Conference on Computer Vision and Pattern Recognition*. IEEE; 2022.
18. Vaswani A, Shazeer N, Parmar N, et al. Attention is all you need. In: *NIPS'17: Proceedings of the 31st International Conference on Neural Information Processing System*. IEEE; 2017:6000-6010.
19. Farha Y, Ke Q, Schiele B, Gall J. Long-term anticipation of activities with cycle consistency. In: *Pattern Recognition: 42nd DAGM German Conference, DAGM GCPR 2020*, Springer; 2020. Accessed July 11, 2025. [https://doi.org/10.1007/978-3-030-71278-5\\_1](https://doi.org/10.1007/978-3-030-71278-5_1)
20. Abu Farha Y, Gall J. Uncertainty-aware anticipation of activities. In: *2019 IEEE/CVF International Conference on Computer Vision Workshop (ICCVW)*. IEEE; 2019:1197-1204.
21. Farha YA, Richard A, Gall J. When will you do what? - Anticipating Temporal Occurrences of Activities. In: *2018*

*IEEE/CVF Conference on Computer Vision and Pattern Recognition.* IEEE; 2018:5343-5352.

22. Gong D, Lee J, Kim M, et al. Future transformer for long-term action anticipation. In: *2022 IEEE/CVF Conference on Computer Vision and Pattern Recognition (CVPR).* IEEE; 2022:3042-3051.

---

## Disclosures

Dr. Tanikawa reported receiving royalties for a patent with TAKAYAMA Instrument, Inc. (Tokyo).

## Author Contributions

Conception and design: Preul, Chen, On, Santello, Li, Xu.  
Acquisition of data: On, Xu, Yangi, Lawton. Analysis and interpretation of data: Chen, On, Xu, Li. Drafting the article: Preul, Chen, On, Xu, Yangi, Santello. Critically revising the article: Preul, Chen, Xu, Tangsrivimol, Lawton, Santello. Reviewed submitted version of manuscript: Chen, Xu, Yangi, Santello, Li. Approved the final version of the manuscript on behalf of all authors: Preul. Statistical analysis: Chen. Administrative/technical/material support: Tanikawa, Li. Study supervision: Li. System implementation, validation, and debugging: Chen.

## Supplemental Information

### Videos

*Video 1.* <https://vimeo.com/1099686676>.

### Correspondence

Mark C. Preul: c/o Neuroscience Publications, Barrow Neurological Institute, St. Joseph's Hospital and Medical Center, Phoenix, AZ. [neuropub@barrowneuro.org](mailto:neuropub@barrowneuro.org).